



EFFECT OF INITIAL FIBER CRACKS ON FRACTURE BEHAVIOR IN CFRP CROSS-PLY LAMINATES

Keiji Ogi*

*Graduate School of Science and Engineering, Ehime University, Japan

Keywords: CFRP, Fiber crack, Fracture behavior, Cross-ply laminate

Abstract

This paper presents characterization of fracture behavior of laminates with initial cracks in fibers. Initial fiber cracks were introduced in prepreg sheets and cross-ply laminates using the cracked prepregs were fabricated. Tensile tests were conducted to obtain the strength and the damage propagation on the top and edge surfaces of the laminate was observed microscopically. Effect of crack geometry on strength and fracture behavior was discussed. The strength of the cracked laminate is proportional to the intact width and independent of crack geometry. Splitting from the initial crack tip, as well as transverse cracking and delamination occurred progressively while fiber breakage takes place just before final failure of the specimen.

1 Introduction

As carbon fiber reinforced plastics (CFRP) have been recently used as large light-weight structures for airplanes, automobiles, mechanical components and reinforcement of buildings etc, assurance of structural reliability has become more essential. In case of applications which require high mechanical performance, continuous carbon fiber composites made of such as prepreg sheets are employed. A number of carbon fibers in those composites could be bended and broken in the vicinity of parts where the radius of curvature is very small. Composite structures fabricated through resin transfer molding (RTM) method may have a bunch of fiber ends according to their cutting patterns of preforms before fabrication. In addition, a sheet molding compound (SMC) made of relatively long discontinuous fiber reinforced plastics is regarded as a sort of a laminate with initial fiber breakage though its fiber orientation is rather random. Although initial fiber damage as well as initial notches [1-3] in composites might cause severe

strength deterioration, little attention has been paid to the strength and fracture behavior of such laminates so far.

The purpose of the present study is to characterize fracture behavior of laminates with initial cracks in fibers. Initial cracks were introduced in prepreg sheets by cutting fibers before fabrication. Cross-ply laminates consisting of the cracked prepregs as longitudinal plies were fabricated. Tensile and fatigue tests were conducted to investigate the static strength as well as fracture behavior of the cracked laminate. Effect of crack geometry such as crack angle and width on strength and fracture behavior was discussed.

2 Experimental Procedure

2.1 Preparation of Specimens

The specimens used are cross-ply laminates of carbon fiber reinforced epoxy (T700S/#2500, Toray) with a stacking sequence of $[0^\circ/90^\circ]_{2S}$. First, initial cracks in CFRP prepreg were introduced by cutting fibers partially as shown in Fig. 1. The fiber cutting angle (crack angle) θ is defined as

$$\theta = \tan^{-1} \frac{W_c}{H_c} \quad (1)$$

where W_c and H_c denote the width and the height of initial cracks, respectively. The initial cracks with a regular spacing of L_c are centered in parallel. Next, four cracked prepreg sheets (0° plies) and another four intact prepreg sheets (90° plies) were stacked. Four kinds of specimens (Specimens IA, IB, II and III) with different combination of W_c , H_c , L_c and θ were fabricated. The values of the geometrical parameters are listed in Table 1. The crack width W_c is determined to be equal to its height H_c only for $\theta = 90^\circ$ in Specimen III. Eight prepreg sheets were stacked so that 0° plies with the crack angle $+\theta$

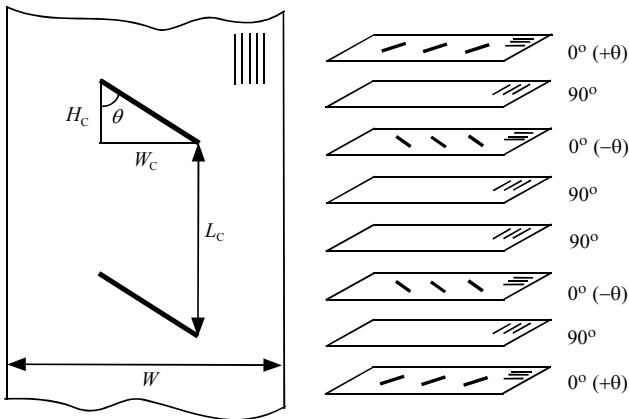


Fig. 1. Geometry and stacking configuration of initially-cracked CFRP cross-ply laminates.

Table 1 Dimensions of specimens (mm).

	IA	IB	II	III
W	20.0	20.0	20.0	20.0
W_c	10.5	13.0	10.5	$H_c \tan \theta$
H_c	$W_c / \tan \theta$	$W_c / \tan \theta$	$W_c / \tan \theta$	10.5
L_c	27.5	27.5	27.5	20
θ	15°, 30°, 45°, 60°, 90°			

and $-\theta$ were alternately inserted except for Specimen II. The crack angle of all the cracked 0° plies is $+\theta$ in Specimen II. Specimens IA and IB have the same crack spacing but different constant crack width. Hence, the crack height varies with the crack angle according to Eq. 1. On the other hand, Specimens IA and II have the same constant crack width but different crack angle as described above. Specimen III has constant crack height and the variable crack width. The crack spacing of Specimen III is also different from that of other specimens. The rectangular specimens with the length of 210 mm and width of 20 mm were cut from the laminate plates and aluminum end tabs were glued on the ends of the specimens for tensile and fatigue tests.

2.2 Loading tests and observation of damage

Tensile tests were conducted with a use of an electrohydraulic testing machine at a loading speed of 49 N/sec and at room temperature. In addition to static tests, fatigue tests were performed only for Specimen II ($\theta = 15^\circ$) under the conditions of the maximum stress of 390 MPa, stress ratio of 0.1 and frequency of 10 Hz.

In order to compare the fracture behavior of the above specimens, the damage progress on the top



Fig. 2. In-situ observation of damage progress on the top surface during a tensile test.

surface was in-situ observed during tensile loading with the use of a video microscope as shown in Fig. 2. The specimen was loaded up to the prescribed maximum load P_{\max} and then unloaded down to P_{UL} ($= 1960$ N). The damage propagating from the initial cracks on the polished top 0° ply was observed at the constant load of P_{UL} . The above procedure was repeated for several P_{\max} until final failure occurs. After the tensile tests and fatigue tests, the top and edge surfaces as well appearance of the specimens was microscopically or macroscopically observed to investigate the damage state at each maximum load and the number of cycles in the tensile and fatigue tests, respectively.

3 Results and Discussion

3.1 Strength

Figure 3 (a) shows tensile strength of all the specimens plotted against crack angle. In Specimens IA, IB and II, where crack angle θ is independent of crack width W_c , the strength is almost insensitive to θ though the slight peak in the strength of Specimen IA is observed at $\theta = 45^\circ$. The strength of Specimen IB is slightly smaller than that of Specimens IA and II. On the other hand in Specimen III, in which W_c changes with θ , the strength decreases with an increase in θ . It should be noted that the strength at $\theta = 45^\circ$ is almost equal to that at $\theta = 90^\circ$ due to definition of W_c in Specimen III. In order to understand the above result, the average strength is plotted against relative crack width in Fig. 3 (b). The strength decreases linearly with increasing relative

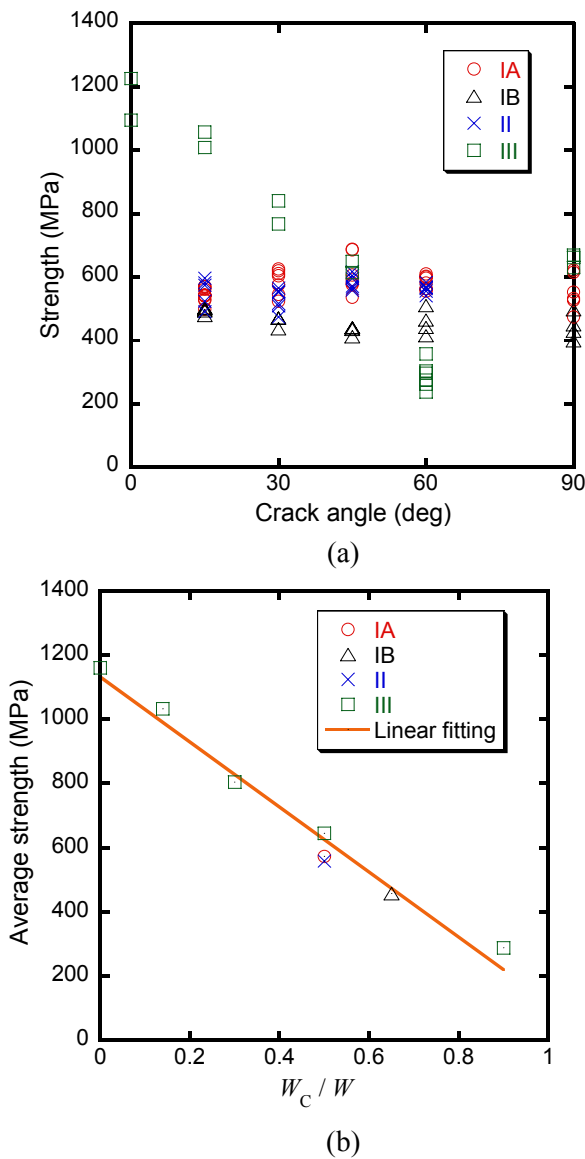


Fig. 3. Effect of (a) crack angle and (b) relative crack width on tensile strength of the cracked cross-ply laminates.

crack width W_c/W . This result is quite reasonable because W_c/W means the ratio of the number of cracked fibers to that of total fibers across the width. Therefore, it is found that failure stress is independent of crack angle and crack spacing in Specimens IA, IB and II with the constant crack width.

3.2 Fracture Behavior

Figure 4 shows appearance of fractured specimens IB after the tensile tests. In Fig. 4 (a), the outer 0° plies are split into pieces. This may be caused by progressive fiber breakage across the width from the tips of initial cracks that follows

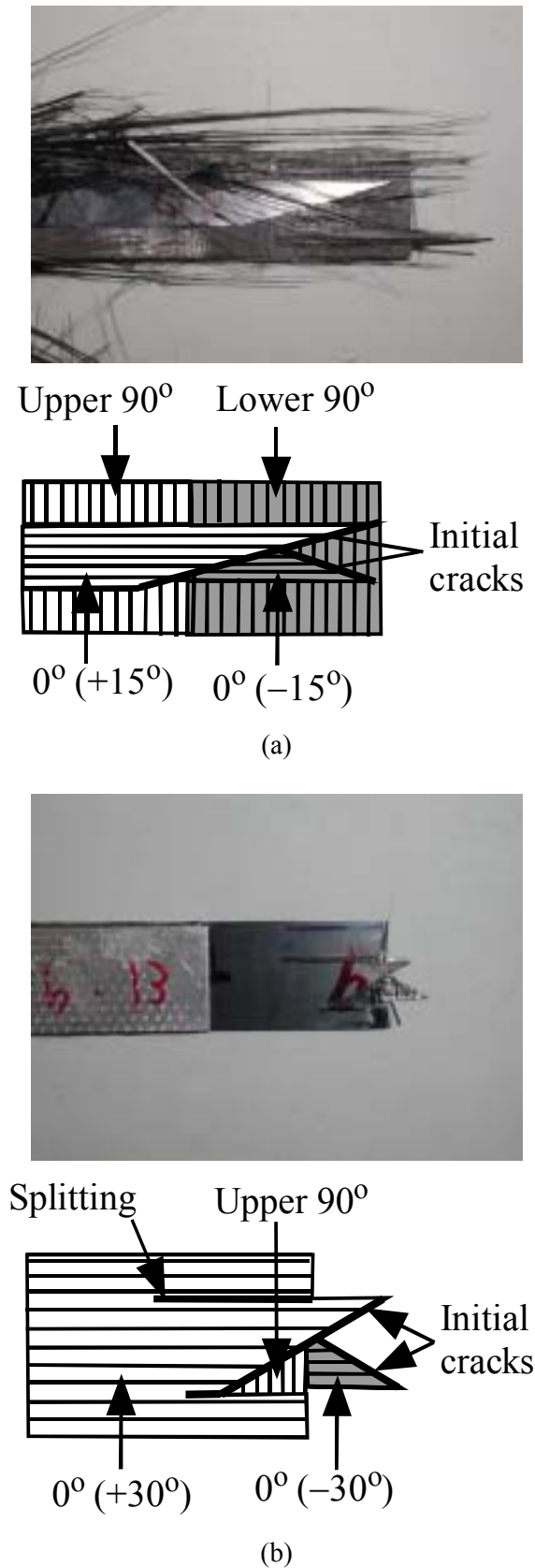


Fig. 4. Fracture behavior in the cracked laminates after the tensile tests of specimens IB with a crack angle of (a) $\theta=15^\circ$, (b) $\theta=30^\circ$ and (c) $\theta=90^\circ$.

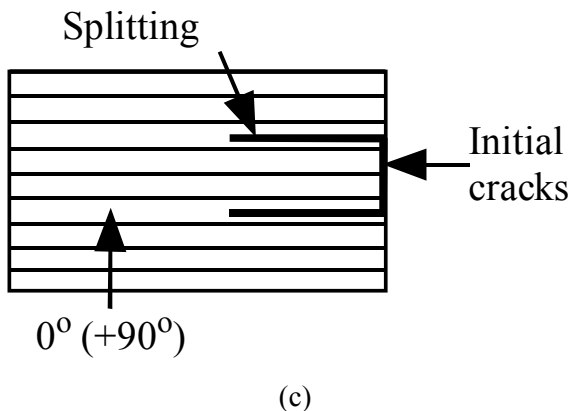
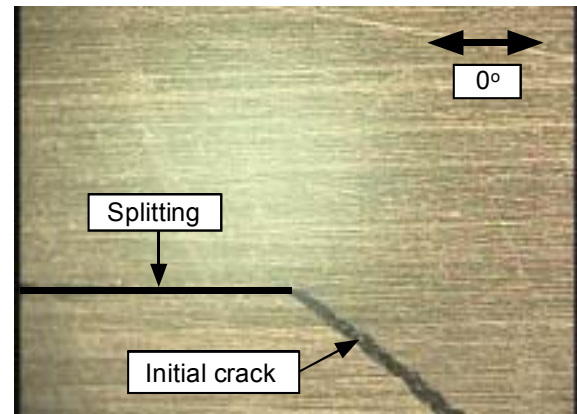


Fig. 4. (continued).

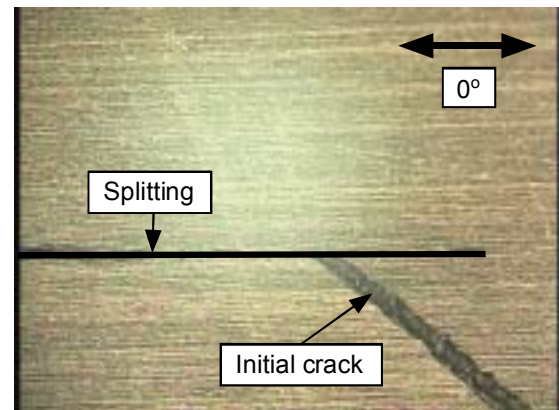
propagation of splitting along the fiber direction. On the other hand, in Fig. 4 (b), the splitting cracks propagate from the tips of the initial cracks in the outer and inner 0° plies along the fiber whilst transverse cracks in the 0° and 90° plies together with delamination are also generated. The main crack propagates along the central line between the two tips of the oblique initial crack. Fracture modes for $\theta = 45^\circ$ and 60° are similar to that for $\theta = 30^\circ$. In Fig.4 (c), splitting and transverse cracking occur from the initial crack tips. Fracture surface is identical to the cross-section on which the initial cracks exist.

Figure 5 shows the damage state in-situ observed on the top surface in specimen IB ($\theta = 45^\circ$). It is observed in all kinds of the specimens that only damage on the top surface generated prior to final failure is splitting crack from the initial crack. Therefore, final failure is presumed to occur just when a main crack in the 0° ply propagates by breaking fibers in a brittle manner. In addition, microscopic observation on the edge views reveals that transverse cracking in 90° plies as well as delamination at the $0^\circ/90^\circ$ interface takes place with increasing load.

Figure 6 shows top surfaces of Specimen II (θ



(a)

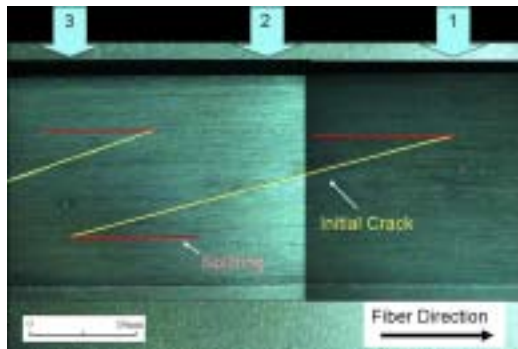


(b)

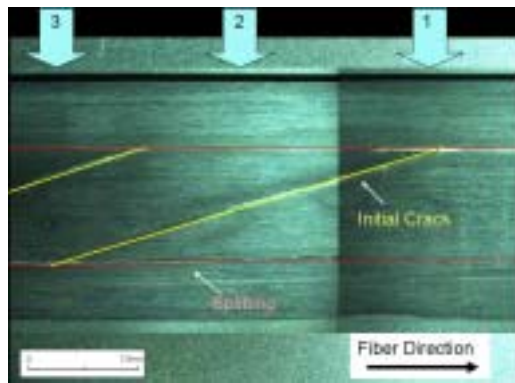
Fig. 5. Damage state observed on the surface in specimen IB ($\theta = 45^\circ$, (a): $\sigma/\sigma_f = 0.62$, (b): $\sigma/\sigma_f = 0.93$, $\sigma_f = 584$ MPa).

$= 15^\circ$) after fatigue loading at two numbers of cycles N ($= 500$ and 10^6). Splitting cracks propagate from the tips of the initial cracks and are connected with each other. Any crack propagation across the width is not observed till final failure.

Figure 7 shows edge surface views of Specimen II ($\theta = 15^\circ$) around the three areas (Area 1, 2 and 3) indicated by the arrows in Fig. 6 after fatigue loading at N of 500 and 10^6 . Transverse cracks and delamination observed in the edge surfaces increase with N (Fig. 7 (a) and (b)). The damage state and degree of damage observed on the edge surface surfaces in Area 1 (Fig. 7 (b)) are proved to be similar to those in Areas 2 and 3 (Fig. 7 (c) and (d)). This result suggests that the effect of initial cracks in the 0° plies on damage progress in 90° plies and the interface is relatively limited. Further investigation on the fracture behavior should be made through numerical stress analysis.

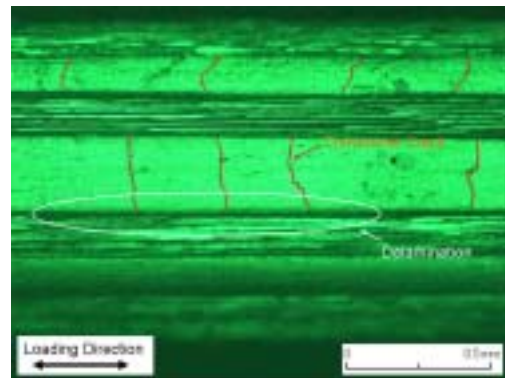


(a)

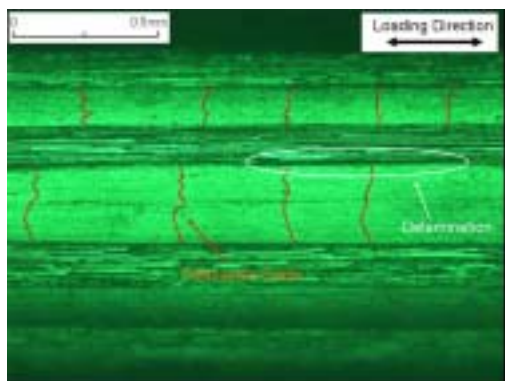


(b)

Fig. 6. Top surface views of Specimen IB ($\theta = 15^\circ$) at N of (a) 500 and (b) 10^6 .

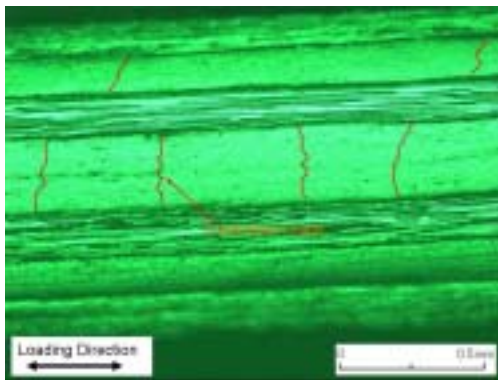


(c)

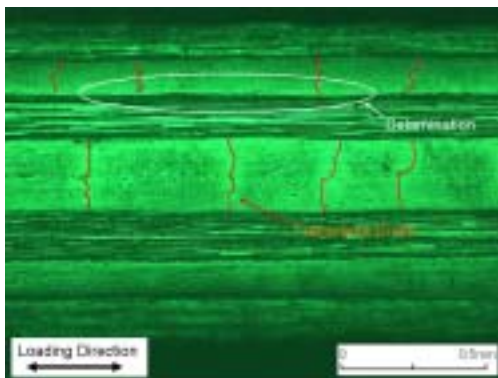


(d)

Fig. 7. Edge views of Specimen IB ($\theta = 15^\circ$) around (a) Area 1 ($N = 500$), (b) Area 1 ($N = 10^6$), (c) Area 2 ($N = 10^6$) and (d) Area 3 ($N = 10^6$).



(a)



(b)

4 Concluding Remark

Strength and fracture behavior of CFRP cross-ply laminates with initial fiber cracks were experimentally studied. Strength of the cracked laminate is proportional to the intact width and independent of crack geometry. Splitting from the initial crack tip as well as transverse cracking and delamination occurs progressively while fiber breakage takes place just before final failure of the specimen.

References

- [1] Chen P., Shen Z., Wang J. Y. "Prediction of the strength of notched fiber-dominated composite laminates". *Compos. Sci. Tech.*, Vol. 61, pp 1311-1321, 2001.
- [2] Olsson R., Iwarsson J., Melin L. G., Sjögren A. and Solti J. "Experiments and analysis of laminates with artificial damage". *Compos. Sci. Tech.*, Vol. 63, pp 199-209, 2003.
- [3] Marissen R., Westphal T. and Sterk J. C. "Fracture of quasi-isotropic composite sheets with sharp notches". *Compos. Sci. Tech.*, Vol. 66, pp 1803-1812, 2006.